cGMP/Protein Kinase G-Dependent Inhibition of N-Type Ca^{2+} Channels Induced by Nitric Oxide in Human Neuroblastoma IMR32 Cells

Marcello D'Ascenzo, Giovanni Martinotti, Gian Battista Azzena, and Claudio Grassi

Institute of Human Physiology, Medical School, Catholic University "S. Cuore", I-00168 Rome, Italy

Although data from our laboratory and others suggest that nitric oxide (NO) exerts an overall inhibitory action on high-voltage-activated Ca^{2+} channels, conflicting observations have been reported regarding its effects on N-type channels. We performed whole-cell and cell-attached patch-clamp recordings in IMR32 cells to clarify the functional role of NO in the modulation of N channels of human neuronal cells. During depolarizing steps to +10 mV from V_h = −90 mV, the NO donor, sodium nitroprusside (SNP; 200 μM), reduced macroscopic N currents by 34% ($p < 0.01$). The magnitude of inhibition was similar at all voltages tested (range, −40 to +50 mV). No significant inhibition was observed when SNP was applied together with the NO scavenger, 2-(4-carboxyphenyl)-4,4,5,5-tetramethylimidazoline-1-oxyl-3-oxide potassium salt (300 μM), or after cell treatment with the guanylate cyclase inhibitor, 1H-[1,2,4] oxadiazole [4,3-a] quinoxalin-1-one (10 μM). 8-Bromoguanosine-cGMP (8-Br-cGMP) (400 μM) mimicked the effects of SNP, reducing Ba^{2+} currents by 37% ($p < 0.001$). Cell treatment with the protein kinase G (PKG) inhibitor KT5823 (1 μM) or guanosine 3′,5′-cyclic monophosphorothioate, 8-(4-chlorophenylthio)-Rp-isomer, triethylammonium salt (20 μM) virtually abolished the effects of 8-Br-cGMP. At the single-channel level, 8-Br-cGMP reduced the channel open probability by 59% and increased both the mean shut time and the null sweep probability, but it had no significant effects on channel conductance, mean open time, or latency of first openings. These data suggest that NO inhibits N-channel gating through cGMP and PKG. The consequent decrease in Ca^{2+} influx through these channels may affect different neuronal functions, including neurotransmitter release.

Key words: nitric oxide; N-type calcium channels; cGMP; protein kinase G; sodium nitroprusside; human neuroblastoma cells

Nitric oxide (NO) is a highly reactive free radical species that acts as a nonconventional intercellular messenger in both the central and peripheral nervous systems. It plays an important functional role in synaptic plasticity phenomena (Schuman and Madison, 1994; Kemenes et al., 2002) and reportedly influences the transmission of sensory information (Haley et al., 1992), including acoustic and proprioceptive signals (Grassi et al., 1995; Azzena et al., 2000). Many of the effects of NO in the nervous system are related to its action on ion channels. This gaseous molecule can spread, in fact, from its site of production and act in adjacent cells, either directly or through second messengers, on various protein substrates, including ion channels. Its influence on Ca^{2+}-activated K^+ channels (Bolotina et al., 1994), Na^+ channels (Li et al., 1998), and Ca^{2+}-activated Cl^- currents (Waniishi et al., 1998) has been well documented, and several reports suggest that it is also involved in the modulation of high-voltage-activated (HVA) Ca^{2+} channels [references in Carabelli et al. (2002)]. In previous studies, we have found that NO donors and cGMP analogs significantly reduce the amplitude of macroscopic currents flowing through both L- and P/Q-type Ca^{2+} channels in rat insulinoma RINm5F cells (Grassi et al., 1999a). More recently, using cell-attached patch recording, we demonstrated that NO also markedly inhibits L-channel gating in bovine chromaffin cells through an increase in intracellular levels of cGMP with consequent activation of protein kinase G (Carabelli et al., 2002).

Although experimental evidence from our laboratory and others suggests that the action of NO on HVA Ca^{2+} channels is predominantly one of inhibition, its specific effects on N-type channels are less clear. Several investigators have suggested that Ca^{2+} influx through these channels is enhanced to some degree by NO donors (Kurenny et al., 1994; Chen and Schofield, 1995; Hirooka et al., 2000). However, more recent findings published by Yoshimura et al. (2001) indicate that, in dorsal root ganglion neurons, NO might actually inhibit N-type Ca^{2+} channels.

These apparently contradictory data prompted us to take a closer look at the effects of NO on N-type Ca^{2+} channels. The present study was conducted at the levels of both macroscopic currents and single channels in an attempt to clarify the nature of the modulatory effects of NO on the N channels of human neuronal cells. We found that the N channels of neuroblastoma IMR32 cells are inhibited by NO, and the mechanism underlying this effect is similar to that described for neuroendocrine L channels (Grassi et al. 1999a; Carabelli et al., 2002); i.e., the effect is mediated by cGMP and protein kinase G (PKG), and it consists of a reduction in the channel open probability and an increase in closed times, which are not associated with significant changes in either channel conductance or mean open time.

The preliminary results of the present study have been published previously in abstract form (Grassi et al., 2000).

Received April 16, 2002; revised June 17, 2002; accepted June 18, 2002.

This research was supported by grants from Ministero dell'Istruzione, dell'Università e della Ricerca and local funds of Catholic University. We thank Daniele Mezzogori for technical assistance.

Correspondence should be addressed to C. Grassi, Institute of Human Physiology, Medical School, Catholic University "S. Cuore", Largo Franceso Vito 1, 00168 Rome, Italy. E-mail: grassi@rm.unicatt.it.

MATERIALS AND METHODS

Cell cultures. Human neuroblastoma IMR32 cells were grown in minimum essential medium (Biochrom KG, Berlin, Germany) supplemented with 10% heat-inactivated fetal bovine serum (HyClone, Logan, UT), 100 IU/ml penicillin, and 100 μg/ml streptomycin (Invitrogen, Grand Island, NY). For electrophysiological recordings, cells were plated at a concentration of $10^4/cm^2$ in 35-mm-diameter plastic Petri dishes and cultured at 37°C in an atmosphere of 5% CO_2 in air. Cell differentiation was induced by 1 mM dibutyryl cAMP and 2.5 μM 5-bromodeoxyuridine (Sigma, St. Louis, MO), which were added to the culture medium three times per week, starting from the day after plating.

Whole-cell recordings. Macroscopic Ba^{2+} currents were recorded using the patch-clamp technique in whole-cell configuration (Hamill et al., 1981) with an Axopatch 200B amplifier (Axon Instruments, Foster City, CA). Electrodes were fabricated from thin-wall borosilicate glass capillaries (Clark Electromedical Instruments, Pangbourne Reading, UK) using a model P-97 Flaming-Brown micropipette puller (Sutter Instruments, Novato, CA), and they were fire polished on a microforge (Narishige Scientific Instrument Laboratory, Tokyo, Japan) before use. The final resistance of the electrode (i.e., after filling with the standard internal solution described below) was 3–5 MΩ. Stimulation and data acquisition were performed with the Digidata 1200 series interface and pCLAMP 6.0.3 software (Axon Instruments). Currents were filtered at 5 kHz with an eight-pole low-pass filter. Capacitative transient and leakage currents were compensated on-line using the clamp-amplifier settings and off-line by subtraction of Cd^{2+}-insensitive (200 μM Cd^{2+}) currents.

Before electrophysiological recordings, the culture medium was removed and replaced with Tyrode's solution containing (in mM): 150 NaCl, 4 KCl, 2 $MgCl_2$, 2 $CaCl_2$, 10 glucose, and 10 HEPES; pH was adjusted to 7.4 with NaOH. The external solution was (in mM): 125 NaCl, 10 $BaCl_2$, 1 $MgCl_2$, 10 HEPES, and 0.0001 tetrodotoxin (TTX) to block Na^+ currents; pH was adjusted to 7.3 with NaOH. The standard internal solution contained (in mM): 110 CsCl, 10 tetraethylammonium chloride (TEA-Cl), 2 $MgCl_2$, 10 EGTA, 8 glucose, 10 HEPES, and, to minimize current rundown during experiments, 4.0 ATP magnesium salt, 0.25 cAMP sodium salt, and 4.0 phosphocreatine disodium salt; pH was adjusted to 7.3 with CsOH.

Solutions containing the different test agents were exchanged by means of a perfusion system consisting of a multibarreled pipette placed within 100 μm of the patched cell and connected to four syringes by means of Teflon tubes. The gravity-regulated flow rate, 0.3–0.5 ml/min, allowed the complete renewal of the extracellular environment in <1 sec. The cell membrane was depolarized every 10 sec (pulse duration, 100–140 msec) at voltages ranging from −40 to +50 mV from the holding potential (V_h) of −90 mV. To isolate HVA currents, each depolarizing pulse was preceded by a 30 msec pulse at −40 mV, which is normally sufficient for complete inactivation of low-voltage-activated (LVA, T-type) Ca^{2+} channels. Unless specified otherwise, the data presented below refer to the effects of test agents on Ba^{2+} currents elicited by depolarization at +10 mV. In some experiments, current density (picoamperes/picoFarads) was estimated by dividing current amplitude by membrane capacitance, measured by the C_{slow} compensation setting of the patch-clamp amplifier.

Cell-attached recordings. Unitary activity of N-type Ca^{2+} channels was recorded in the cell-attached configuration (Hamill et al., 1981) using the Axopatch 200B amplifier. Electrodes were pulled from thick borosilicate glass capillaries (Hilgenberg, Mansfield, Germany) and coated with Sylgard 184 (Dow Corning Corporation, Midland, MI). Their final resistance (after filling with the recording solution) ranged from 4 to 9 MΩ. The pipette solution contained (in mM): 100 $BaCl_2$, 10 TEA-Cl, 1 $MgCl_2$, 10 Na-HEPES, 0.0003 TTX, and 0.005 nifedipine for blockade of L-type channels (pH adjusted to 7.3 with TEAOH). The cell-attached condition was achieved with the cell bathed in Tyrode's solution. Membrane potential was zeroed by perfusing the cell with a control solution containing (in mM): 135 KAsp, 1 $MgCl_2$, 10 HEPES, 5 EGTA, and 0.0003 TTX (pH adjusted to 7.3 with KOH). The perfusion system described above was used for exchange of drug-containing solutions.

Current traces were acquired at 10 kHz and filtered on-line at 2 kHz. Membrane stimulation and data acquisition were performed with pCLAMP software. N-channel activity was recorded after delivery of 120–500 msec depolarizing pulses at +10, +20, and +30 mV from V_h = −80 mV. Consecutive depolarizations were applied every 6 sec for 6–10 min. For all groups of experiments, the data shown refer to the first 6 min recording: the first minute under control conditions followed by 5 min in the presence of the test drugs.

Data analysis. Data were analyzed with TAC and TACFIT software (version 3.04; Bruxton Corporation, Seattle, WA). Fast capacitative transients were minimized on-line by means of patch-clamp analog compensation. Uncorrected capacitative currents were eliminated by averaging sweeps with no channel activity (nulls) and subtracting them from each active sweep. Event detection was performed with the 50% threshold detection method, and each transition was visually inspected before being accepted.

In experiments performed to evaluate the effects of 8-bromoguanosine-cGMP (8-Br-cGMP) on the channel open probability, data analysis also included patches in which the activity of more than one channel was recorded. In these multichannel patches (n = 7), the open probability, indicated as NPo, was calculated by adding the duration of single, double, and even triple openings and dividing the sum by the duration of the analyzed time interval (Lambert and Feltz, 1995). In evaluation of the NPo, the first and the last closures were excluded; analyses were made with and without inclusion of null sweeps. Mean NPo values were obtained by averaging the data collected over 30 sec periods. Changes in the null sweep probability during application of 8-Br-cGMP were also estimated.

Patches containing unitary openings (n = 5) were used to study the effects of 8-Br-cGMP on the single-channel open probability (Po), mean open time, mean closed time, and latency of the first opening at +20 mV. In this group of experiments, depolarizing pulses lasting 500 msec were used to obtain better resolution of the longest closed time component. The Po was evaluated, as described above, after exclusion of the first and last closures. Histograms representing open and closed times were plotted on square root-log coordinates and constructed as described previously (Carabelli et al., 2002). Data were not corrected for missed events, and the distributions of open and closed times were fitted by the sum of decaying exponential. As far as the open time distribution is concerned, unitary data events from patches containing more than one channel were also included in the analysis to increase the number of studied events. The mean amplitude of the unitary current was determined by fitting the amplitude histograms with a Gaussian distribution. The unitary conductance was evaluated by linear regression of the mean unitary currents recorded at voltages ranging from +10 to +30 mV.

All of the experiments were performed at room temperature (22–24°C). Data are presented as means ± SEM. Student's t test was used for statistical analysis, and p values <0.05 were considered significant. The statistical significance of NPo changes observed during cell exposure to 8-Br-cGMP was assessed by ANOVA for repeated measurements.

In experiments aimed at evaluating the effects of the NO donor, sodium nitroprusside (SNP), the drug was added to the external solution, and the cell preparation was exposed to a fiber-optic light to induce NO production from SNP breakdown (Bates et al., 1991). In the preliminary phase of the study, the possible effects of this light on the recorded currents (caused by the breakdown of nifedipine in the external solution) were specifically excluded. Current amplitude and kinetics in 5 min recordings obtained while the light was on were not significantly different from those of control recordings made before switching on the light (data not shown). After each trial in which SNP or analogs/antagonists of the NO-induced second messengers were used, the culture dish was replaced, and further recordings were obtained from cells that had not been challenged previously with any drugs.

Drugs and solutions. The following compounds were used: SNP (20–200 μM, Sigma), 2-(4-carboxyphenyl)-4,4,5,5-tetramethyl-imidazoline-1-oxyl-3-oxide potassium salt (carboxy-PTIO, 300 μM; Affiniti Research Products, Mamhead, UK), 8-Br-cGMP (400 μM; Sigma), 1H-[1,2,4] oxadiazole [4,3-a] quinoxalin-1-one (ODQ, 10 μM; Alexis Corporation, Läufelfingen, Switzerland), KT5823 (1 μM); guanosine 3′,5′-cyclic monophosphorothioate, 8-(4-chlorophenylthio)-Rp-isomer, triethylammonium salt (Rp-8-pCPT-cGMPS, 20 μM) (Calbiochem, CN Biosciences, Darmstadt, Germany), and ω-conotoxin-GVIA (ω-CTx-GVIA, 3.5 μM; Alomone Labs, Jerusalem, Israel). Nifedipine (5 μM, Sigma) was diluted before each experiment from 1 mM stock solution in ethanol, which was stored in the dark at 4°C.

RESULTS

Effect of the NO donor SNP on macroscopic N-type currents

Human neuroblastoma IMR32 cells express various types of HVA Ca^{2+} channels as well as LVA (T-type) channels, which are found with variable frequency during the first days of cell differ-

entiation (Carbone et al., 1990; Grassi et al., 1994). To isolate LVA currents, each depolarizing stimulus (−40 to +50 mV) was preceded by a 30 msec prepulse at −40 mV from $V_h = -90$ mV (see Materials and Methods). This stimulation protocol allowed us to segregate the HVA currents, and the relative contributions of the channel types could then be identified by means of pharmacological blockade.

During depolarization at +10 mV, blockade of L-type channels by nifedipine (5 μM) reduced the peak HVA current by 10.0 ± 2.4% ($n = 17$) with respect to controls, and the residual Ba^{2+} current was further diminished (reduction of ≥90%) by the application of 3.2 μM ω-CTx-GVIA, which is a selective blocker of N channels (Kasai et al., 1987). To confirm these findings, a second set of experiments was performed in which current densities were measured in controls and in cells pretreated for 10 min with 3.2 μM ω-CTx-GVIA. Nifedipine (5 μM) was used in both groups to maintain L-channel blockade. In the presence of both nifedipine and ω-CTx-GVIA, current density was 3.8 ± 1.1 pA/pF ($n = 5$) as opposed to 36.3 ± 4.5 pA/pF ($n = 10$) in controls treated with nifedipine alone. These results demonstrate that, under conditions of L-channel blockade, almost all of the HVA Ba^{2+} current (~90%) in IMR32 cells is carried through N-type Ca^{2+} channels.

This preparation was considered a good experimental model for investigation of NO-induced modulation of human N-type channels. Therefore, all of the data reported below were collected in experiments in which the occasional T-type current had been eliminated by means of prepulse depolarization and L channels had been blocked by 5 μM nifedipine.

Cell exposure to the NO donor, SNP (200 μM), consistently reduced HVA Ba^{2+} currents, whereas T-type currents, when present, were not significantly affected (Fig. 1). The SNP-induced effects appeared with a latency of 10–20 sec, and the maximal decrease was reached after 4–5 min of exposure. With respect to controls, the current was reduced by 34.1 ± 1.5% ($n = 21$; $p < 0.01$) after 3 min of SNP exposure and by 46.9 ± 1.6% ($p < 0.001$) 2 min later. After the removal of SNP, either there was a partial recovery (ranging from 7 to 14% of values measured at the end of drug exposure) or the current amplitude remained quite stable for 1–2 min during washout with standard external solution (Fig. 1*B*,*C*). Lower SNP concentrations (20 μM) produced milder inhibition (14.8 ± 1.1% current reduction; $n = 7$), and recovery during washout seemed to be somewhat more substantial, although given the limited inhibition produced and the amount of current rundown, this difference is not easy to quantify.

Current activation and inactivation kinetics were not significantly affected by SNP. Time to peak at +10 mV was, in fact, 6.9 ± 0.5 msec ($n = 9$) in controls and 6.5 ± 0.6 msec in cells treated with the NO donor. The inactivation time constant at the same voltage was 58.3 ± 1.5 msec in controls and 58.6 ± 1.5 msec in the presence of SNP. Current inhibition in the same order of magnitude was induced by SNP at all voltages tested, and there was no significant shift in the peak of the current–voltage (*I–V*) relationship (Fig. 2).

To verify the specificity of the effects of SNP, we also evaluated current rundown under our experimental conditions. Recordings of 6–8 min with the standard external solution, without addition of any drugs, revealed that the current amplitude remained stable for the first 3 min (95.1 ± 2.1% of controls; $n = 5$) and decreased slightly (to 88.6 ± 4.0% of the control values) during the following 2 min. To minimize the possible confounding effects of current rundown in whole-cell recordings, we therefore chose to quantify the effects of all test compounds after 3 min of exposure. This approach, however, probably resulted in underestimation of the inhibitory effects of the NO donor and related compounds, and for this reason maximal effects observed after 5 min are also reported in most cases. Unless specified otherwise, the reported data refer to effects estimated at the end of the third minute of exposure to the test agent.

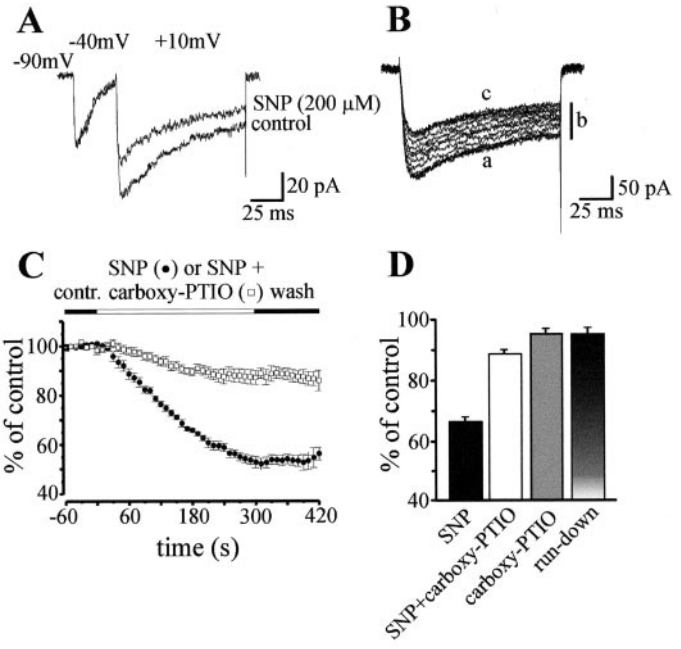

Figure 1. The NO donor sodium nitroprusside (*SNP*) (200 μM) markedly reduces whole-cell Ba^{2+} currents through N-type channels in nifedipine (5 μM)-treated human neuroblastoma IMR32 cells. *A*, Representative traces showing SNP effects on low-voltage- and high-voltage-activated currents elicited by step depolarization at +10 mV preceded by a 30 msec prepulse at −40 mV from $V_h = -90$ mV. *B*, Time course of SNP effect on N-type current (traces during prepulse at −40 mV are not shown, and only recordings during depolarization at +10 mV are presented): *a*, control; *b*, current amplitude is progressively reduced throughout 3 min cell exposure to SNP (traces at 30 sec intervals are shown); *c*, after the end of SNP application, modest recovery occurs during 2 min washout with standard external solution. *C*, The percentage changes in current amplitude are plotted against time during application of either 200 μM SNP (●) or 200 μM SNP together with the NO scavenger carboxy-PTIO (300 μM; □). Data shown are averages (±SEM) of currents normalized with respect to the control amplitude ($n = 9$ in each group). *D*, Changes in peak current amplitude at the third minute of cell exposure to 200 μM SNP ($n = 21$), 200 μM SNP together with 300 μM carboxy-PTIO ($n = 5$), 300 μM carboxy-PTIO alone ($n = 5$), or standard external solution without addition of any drugs ($n = 5$).

Application of 200 μM SNP together with the NO scavenger carboxy-PTIO (300 μM) failed to significantly reduce N-type current, providing further evidence of the specificity of the action of NO (Fig. 1*C*,*D*). Peak current amplitude in the presence of these two compounds was, in fact, 88.5 ± 1.5% ($n = 5$) of controls. This value was significantly different ($p < 0.001$) from that observed when the cells were exposed to SNP alone, whereas it was not significantly different from that produced by current rundown. Cell exposure to carboxy-PTIO alone had no significant effect on peak current amplitude (95.1 ± 1.9%, $n = 5$) (Fig. 1*D*).

The results of this first group of experiments suggest that the N-type Ca^{2+} current inhibition induced by SNP is a specific

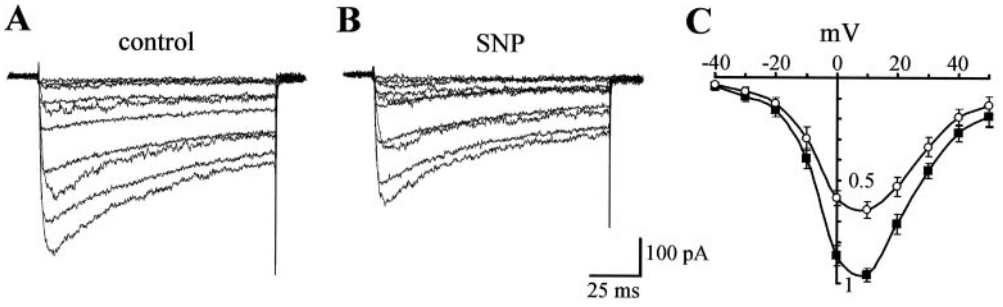

Figure 2. The magnitude of SNP-induced inhibition is similar at all voltages tested. *A*, *B*, Representative traces recorded during depolarization at voltages ranging from −40 mV to +50 mV in control and during application of 200 μM SNP. As in Figure 1*B*, current recordings during prepulse at −40 mV are not shown. *C*, Current–voltage relationships in control (■) and in the presence of SNP (○) were obtained by averaging data from $n = 7$ cells. In each cell, current amplitudes at the different potentials are normalized to the peak current value at time 0 (=1), expressed in arbitrary units.

effect of NO itself, unrelated to the actions of other SNP breakdown products or current rundown.

Second messengers mediating the NO-induced inhibition of N channels

We then attempted to determine whether the observed decrease in current amplitude was caused by a direct action exerted by NO on N-type Ca^{2+} channels or the result of an increase in the intracellular levels of cGMP, which is known to mediate many biological effects of NO. In cells pretreated for 15 min with the potent and selective guanylate-cyclase inhibitor ODQ (10 μM) (Garthwaite et al., 1995), subsequent exposure to 200 μM SNP and 10 μM ODQ reduced Ba^{2+} currents by only 10.6 ± 3.0% ($n = 5$), suggesting that guanylate cyclase activity is necessary for the action of SNP (Fig. 3). The involvement of cGMP production in the observed N-current reduction was also supported by the results of experiments with the membrane-permeant cGMP analog, 8-Br-cGMP. At a concentration of 400 μM, 8-Br-cGMP mimicked the effects of SNP, reducing Ba^{2+} currents by 37.2 ± 3.7% ($n = 7$; $p < 0.001$) after 3 min and by 51.6 ± 1.7% after 5 min. In cells pretreated for 20 min with the specific PKG inhibitor KT5823 (1 μM) (Grider, 1993), the application of 8-Br-cGMP together 1 μM KT5823 produced a much more limited reduction in N-channel currents (13.4 ± 2.6%; $n = 9$). Similar results were obtained with another PKG inhibitor, Rp-8-pCPT-cGMPS (Ropero et al., 1999). Combined exposure to 400 μM 8-Br-cGMP and 20 μM Rp-8-pCPT-cGMPS of cells that had already been incubated with the same PKG inhibitor (20 μM) for 30 min reduced N-current amplitude by only 8.5 ± 3.9% ($n = 5$). In the absence of 8-Br-cGMP, neither KT5823 nor Rp-8-pCPT-cGMPS had any significant effect on the amplitude of Ba^{2+} currents.

Single-channel parameters affected by cGMP

The previous groups of experiments showed that macroscopic N currents are markedly inhibited by NO via the cGMP/PKG pathway. To identify the single-channel parameters affected by this second-messenger cascade, we then reinvestigated the effects of 8-Br-cGMP in cell-attached patches of IMR32 cells. Step depolarization at +20 mV from $V_h = -80$ mV was delivered every 6 sec, and pipette solutions contained 100 mM $BaCl_2$ and 5 μM nifedipine. In the presence of the L-channel blocker, N-channel activity could be recorded and clearly distinguished from that of other channels that might be found in the patch, using criteria reported in the literature (Carabelli et al., 1996; Elmslie, 1997). Data collected from patches in which non-N-type activity was present were excluded from analysis. Before actual experiments, 6–8 min recordings were made under control conditions in three patches. As shown in Figure 4, N-channel activity remained stable, with no significant changes in the channel open probability.

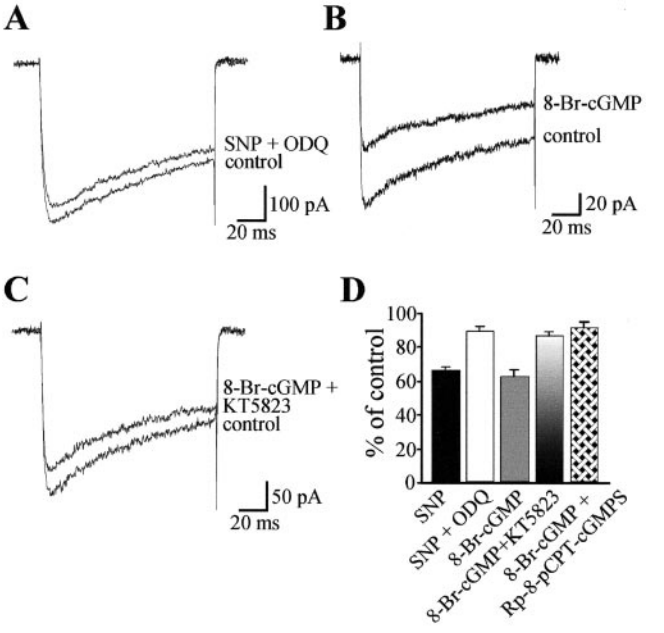

Figure 3. N-channel inhibition by NO is mediated by cGMP and protein kinase G. *A*, The effect of 200 μM SNP is prevented by the guanylate cyclase inhibitor ODQ (10 μM). *B*, Application of the membrane-permeant cGMP analog, 8-Br-cGMP (400 μM), mimics SNP effect, markedly reducing Ba^{2+} currents. *C*, In the presence of the PKG inhibitor KT5823 (1 μM), 8-Br-cGMP only slightly reduces N-channel currents. *D*, Percentage decrease in the peak-current amplitude measured at the third minute of cell exposure to 200 μM SNP alone ($n = 21$), 200 μM SNP in the presence of 10 μM ODQ ($n = 5$), 400 μM 8-Br-cGMP ($n = 7$), and 400 μM 8-Br-cGMP after cell treatment with either 1 μM KT5823 ($n = 9$) or 20 μM Rp-8-pCPT-cGMPS ($n = 5$). All data shown have been collected in IMR32 cells treated with 5 μM nifedipine during depolarization at +10 mV after prepulse at −40 mV (current traces during prepulse are not shown).

When the effects of 8-Br-cGMP were tested, the cGMP analog (400 μM) was applied through the external "zeroing" solution after a 1 min recording under control conditions, and the activity of available channels was usually evaluated during the following 5 min. Extracellular application of 8-Br-cGMP markedly reduced the open probability of N channels (Fig. 4). In some of the patches ($n = 7$), the activity of two or three Ca^{2+} channels was recorded ($n = 4$ and $n = 3$, respectively), and in these cases the open probability was evaluated as NPo (see Materials and Methods). In particular, mean NPo values were obtained by averaging data collected over 30 sec periods. The decrease in NPo induced by 8-Br-cGMP was characterized by a variable latency (10–50 sec), and the peak effect was usually reached in the following 2–3 min. Under control conditions, the mean NPo was 0.27 ± 0.05 ($n = 7$),

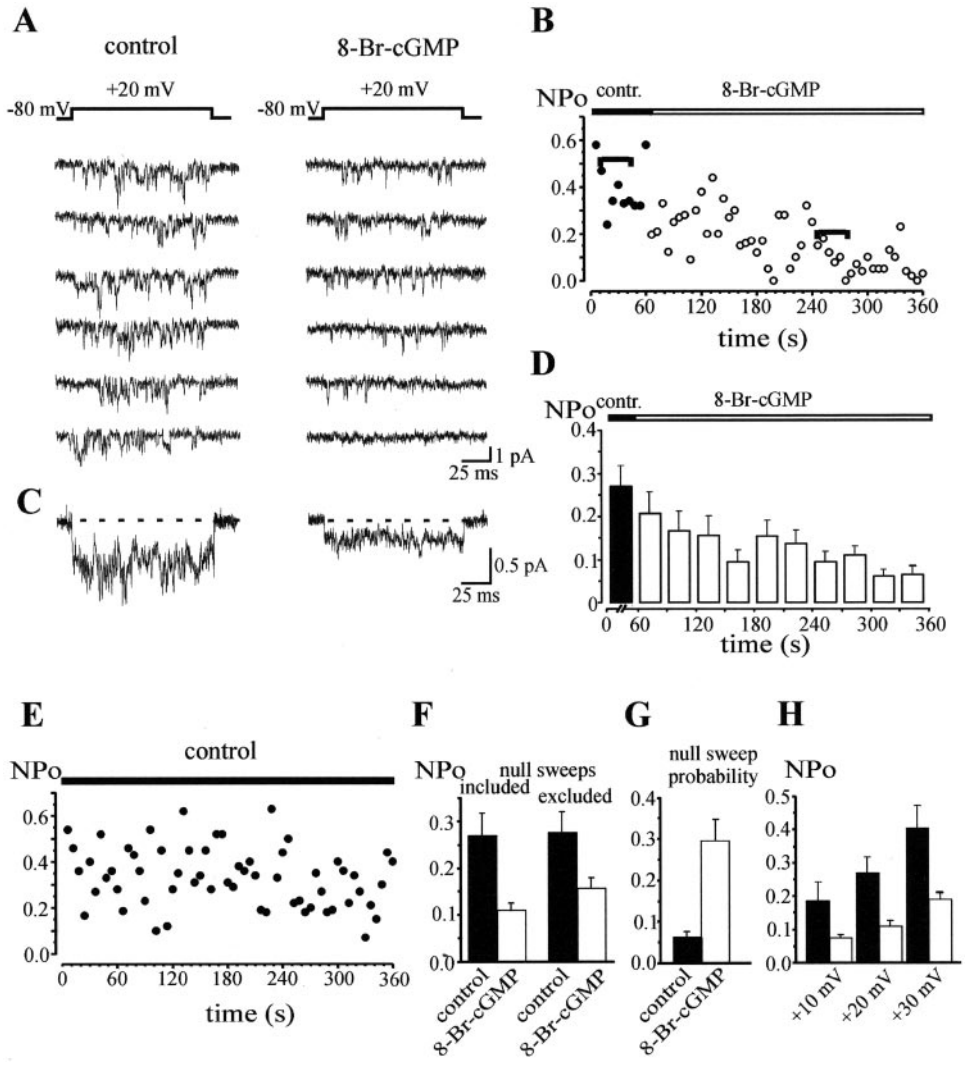

Figure 4. 8-Br-cGMP markedly reduces the open probability of N channels in human neuroblastoma cells. *A*, Representative traces of N-channel activity recorded in a cell-attached patch containing more than one channel under control conditions (*left*) and during exposure to 400 μM 8-Br-cGMP (*right*). Nifedipine (5 μM) was present in the pipette solution to block L channels, and depolarization at +20 mV was delivered from $V_h = -80$ mV. *B*, NPo versus time before (●) and during application of 8-Br-cGMP (○). Data plotted refer to the same patch shown in *A*, and *horizontal bars* indicate the selected traces presented in *A*. *C*, Averaged currents calculated over 10 sweeps in control and 40 sweeps with 8-Br-cGMP from the same patch shown in *A* and *B*. *D*, Mean changes in NPo induced by 400 μM 8-Br-cGMP in seven patches containing two or three N channels. *Filled column* shows NPo value obtained by averaging data collected during 1 min recording under control conditions before application of the test agent. The *open columns* indicate mean NPo obtained by averaging the data collected in the seven studied patches over 30 sec periods. *E*, NPo versus time for a representative patch recorded under control conditions (i.e., in absence of test drugs) shows the absence of significant rundown. Mean NPo is 0.37 ± 0.04 during the first minute and 0.33 ± 0.02 during the second through the sixth minutes. *F*, The 8-Br-cGMP-induced decrease in NPo is estimated with and without inclusion of null sweeps (59.3 and 42.9% reduction, respectively). In *F–H*, *filled columns* indicate controls obtained by averaging data collected during 1 min recordings, and *open columns* show values obtained by averaging all the data collected from the second to the fifth minute of drug application. *G*, Marked increase in null sweep probability induced by 8-Br-cGMP with respect to control (0.29 ± 0.04 vs 0.06 ± 0.03). *H*, Mean values of NPo at +10, +20, and +30 mV, the percentage decrease induced by 8-Br-cGMP being 60.3, 59.3, and 52.9%, respectively.

and its reduction was statistically significant after the first minute of 8-Br-cGMP exposure ($F_{(2,6)} = 9.48$; $p < 0.01$). The mean NPo in the presence of 8-Br-cGMP was thus calculated on the basis of data collected from the second through the fifth minutes of exposure. The result (0.11 ± 0.01) represented a 59.3% reduction with respect to controls ($p < 0.001$). The averaged current during cell exposure to 8-Br-cGMP was smaller in amplitude with respect to control, but it exhibited a similar time course (Fig. 4*C*). A smaller, but still significant, NPo decrease (42.9%; i.e., from 0.28 ± 0.05 to 0.16 ± 0.02; $p < 0.01$) was also found when this parameter was plotted over time after exclusion of null traces (Fig. 4*F*). The null sweep probability was significantly increased, in fact, from 0.06 ± 0.03 to 0.29 ± 0.04 ($p < 0.01$) during cell exposure to 8-Br-cGMP (Fig. 4*G*). The magnitude of the inhibitory action of 8-Br-cGMP was similar at voltages ranging from +10 to +30 mV (Fig. 4*H*).

Channel conductance, evaluated by measuring current amplitudes at voltages ranging from +10 to +30 mV, was not significantly affected by 8-Br-cGMP application (slope conductance: 20.2 ± 0.6 pS in the presence of the cGMP analog and 19.4 ± 2.4 pS in controls) (Fig. 5). In particular, current amplitudes under control conditions and during application of 8-Br-cGMP were, respectively, −1.35 ± 0.03 and −1.34 ± 0.04 pA at +10 mV ($n = 4$), −1.10 ± 0.03 and −1.12 ± 0.04 pA at +20 mV ($n = 7$), and −0.95 ± 0.02 and −0.93 ± 0.01 pA at +30 mV ($n = 4$). The amplitude distribution at +20 mV in controls and 8-Br-cGMP-exposed cells is shown in Figure 5*A*.

Plots of the open time distribution were fitted according to one exponential with $\tau_o = 1.12$ msec in controls and 1.19 msec during 8-Br-cGMP application. Arithmetic means of open times were 1.28 ± 0.02 msec in controls and 1.37 ± 0.03 msec in the presence of 8-Br-cGMP when all data from 12 patches were pooled and 1.26 ± 0.07 msec and 1.35 ± 0.13 msec, respectively, when mean values obtained from each patch ($n = 12$) were averaged.

In five patches, in which only single-channel activity was recorded, Po, shut time, and latency of first opening were studied during 500 msec depolarization at +20 mV. 8-Br-cGMP decreased the Po by 54.5% (0.05 ± 0.01 vs 0.11 ± 0.01; $p < 0.001$) (Fig. 5*D*), and this reduction was not very different from the NPo decrease reported above (59.3%), thus suggesting that 8-Br-cGMP mainly affects N-channel gating (Po) rather than the number of available channels. In fact, most of its effects on Po are attributable to an increase in the null sweep probability together with a prolongation of closed times (Fig. 5*E*,*F*). The closed time

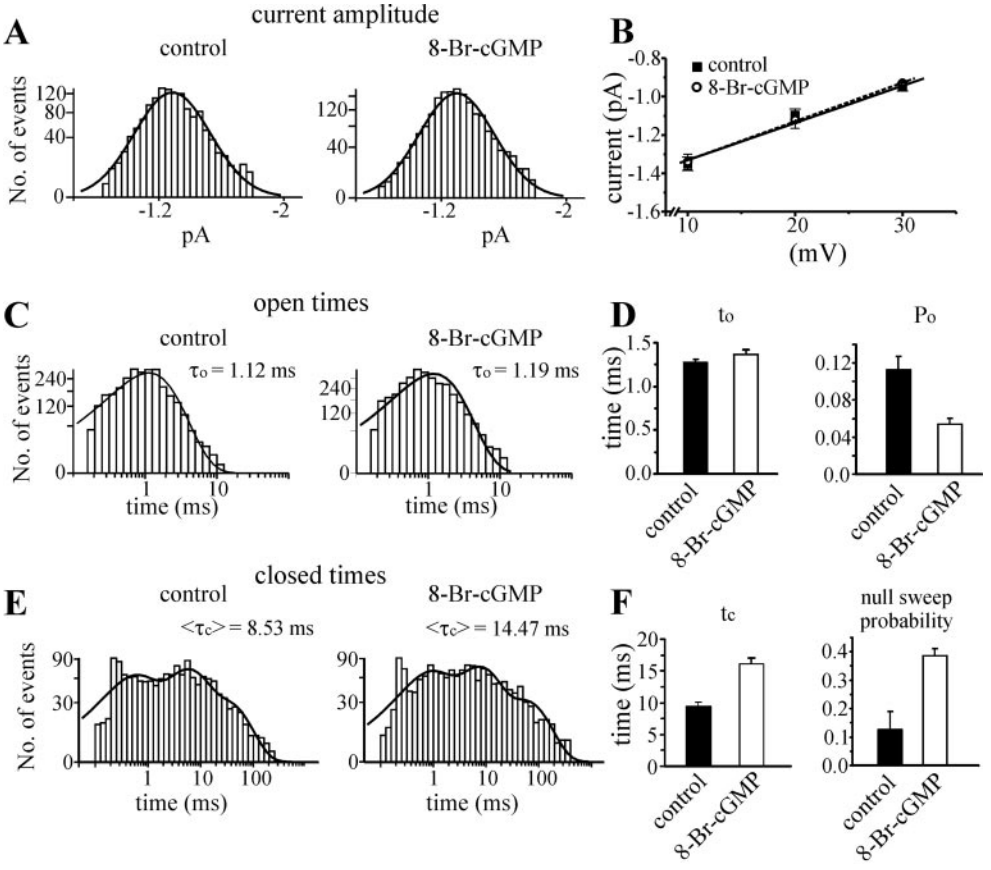

Figure 5. Single N-channel parameters in control and during application of 8-Br-cGMP. *A*, Histogram distribution of single N-channel amplitudes measured at +20 mV in control and with 8-Br-cGMP: the mean amplitudes are −1.10 ± 0.03 and −1.12 ± 0.04 pA, respectively. *B*, Mean unitary current amplitudes plotted versus voltage. The linear regression through data points have mean slope conductances of 19.4 ± 2.4 pS in control and 20.2 ± 0.6 pS in the presence of the cGMP analog. *C*, Open time distribution at +20 mV. The distributions were fitted with one exponential function with τ_o = 1.12 msec in control and 1.19 in the presence of 8-Br-cGMP. *D*, Effects of 8-Br-cGMP on the mean open time (t_o) obtained from the arithmetic mean of all data collected (1.37 ± 0.03 vs 1.28 ± 0.02 in controls) and on Po obtained from patches containing single N channel only (0.05 ± 0.01 vs 0.11 ± 0.01; 54.5% decrease). *E*, Closed time distribution at +20 mV is fitted with a three-exponential function with the following time constants: τ_{C1} = 0.45 msec (34.1%), τ_{C2} = 4.86 msec (43.1%), and τ_{C3} = 27.51 msec (22.8%) in controls and τ_{C1} = 0.66 msec (33.1%), τ_{C2} = 6.55 msec (45.1%), and τ_{C3} = 51.83 msec (21.8%) with 8-Br-cGMP. The mean $<\tau_C>$ values derived from the fit (8.53 msec in controls and 14.47 msec with 8-Br-cGMP) are given on the *top* of each distribution, and they compare well with those derived by the arithmetic mean of the collected data shown in *F* (t_c = 9.44 ± 0.67 msec in controls and 16.08 ± 0.94 msec with 8-Br-cGMP). *F*, Besides changes in t_c, the increase in null sweep probability induced by 8-Br-cGMP in single N-channel recording is shown (0.13 ± 0.06 vs 0.39 ± 0.02).

distribution was fitted with a three-exponential function, all time constants being significantly prolonged by the cGMP analog. The mean τ_C values derived from the fit (8.53 msec in controls, 14.47 msec with 8-Br-cGMP) compared well with those derived by averaging the closed times of all studied patches (9.44 ± 0.67 msec in controls, 16.08 ± 0.94 msec with 8-Br-cGMP). This finding reinforced the view that the prolongation of mean τ_C is one of the main causes of the Po decrease induced by the cGMP analog.

The latency of first openings was not significantly affected by 8-Br-cGMP (18.6 ± 2.8 msec vs 18.7 ± 3.8 msec in controls).

DISCUSSION

In the present paper, we show that NO markedly inhibits N-type Ca^{2+} channels in human neuroblastoma IMR32 cells by inducing an increase in intracellular levels of cGMP with consequent activation of protein kinase G. The SNP-induced decrease in the amplitude of macroscopic N-type currents was prevented, in fact, by the guanylate cyclase inhibitor ODQ, mimicked by membrane-permeant cGMP, and virtually abolished by different PKG inhibitors. The specificity of these effects is confirmed by the absence of significant changes in current amplitude after application of SNP together with the NO scavenger carboxy-PTIO, as well as by the marked difference between SNP-induced inhibition and current rundown over the same time period. The SNP-induced inhibition was voltage independent, as shown by the similar magnitude of current reduction observed at the different voltages tested. The time course of the effects and the limited recovery observed during the first 2 min of washout are consistent with the reports of various investigators (Chen and Schofield, 1995; Chik et al., 1995; Tewari and Simard, 1997; Lang et al., 2000). At the single-channel level, the inhibitory action of cGMP consists of a reduction of the open probability of available channels and an increase in the mean closed time. The latency of first openings, mean open times, and channel conductance are not significantly influenced. The inhibitory effect of the cGMP analog on the channel open probability (54–59% inhibition) was slightly greater than that observed on macroscopic current amplitude after application of SNP or 8-Br-cGMP (reductions ranging from 34 to 52% of controls with the different tested agents at the third and the fifth minutes of drug application, respectively). This difference might be related to cell dialysis during whole-cell recordings, which could reduce the effectiveness of intracellular second messengers produced by NO donors. In chick ciliary ganglion neurons, Ca^{2+} current inhibition induced by somatostatin and cGMP agonists differed under perforated-patch and whole-cell conditions, and the loss or inhibition of cGMP-dependent protein kinase in the latter experimental condition was suggested as a possible cause of these differences (Meriney et al., 1994).

Data reported in this paper represent the first experimental evidence that the NO-induced second-messenger cascade inhibits N-type Ca^{2+} channels by affecting channel gating. Similar effects are induced by NO donors and cGMP in L-type channels of neuroendocrine cells. In rat insulinoma RINm5F cells, SNP dose-dependently reduces HVA Ca^{2+} currents (Grassi et al., 1999a). Moreover, in single L channels of bovine chromaffin cells, exposure to either 200 μM SNP or 400 μM 8-Br-cGMP is followed

by a decrease of nearly 60% in Po (Carabelli et al., 2002). The findings that emerge from the present study also fit nicely with the NO-induced inhibition of L-type Ca^{2+} channels that has been observed in various experimental models, although the mechanisms responsible for these effects may be different. NO has been reported to inhibit Ca^{2+} channels either through a direct action consisting in *S*-nitrosylation of the channel protein (Hu et al., 1997; Summers et al., 1999) or by activating guanylate cyclase. The increase in cGMP levels can produce channel inhibition through activation of phosphodiesterase, with consequent downregulation of the cAMP/PKA-activating pathway or through protein kinase G [see references in Carabelli et al. (2002)].

Our findings indicate that this latter mechanism is responsible for the NO-induced inhibition of both neuronal N channels and neuroendocrine L channels. Although most of the published data indicates that NO inhibits Ca^{2+} currents, a few reports have suggested that N channels might actually be facilitated by this intracellular messenger. In particular, Chen and Schofield (1995) reported that NO increases Ca^{2+} current amplitude in rat sympathetic neurons. However, it should be noted that although high extracellular concentrations (500 μM) of the NO donors SNP and (±)*S*-nitroso-*N*-acetyl-penicillamine (SNAP) were used in this study, macroscopic currents were enhanced by only 9.9 ± 3.0% and 16.6 ± 3.7%, respectively. The effects of SNP were approximately halved by application of the guanylate cyclase inhibitor, methylene blue, thus suggesting an involvement of cGMP in the observed responses. Hirooka and coworkers (2000) reported a 21–23% increase in the macroscopic Ba^{2+} currents of salamander retinal ganglion cells exposed to high concentrations (1 mM) of SNAP. This effect was mimicked by the cGMP analog, CPT-cGMP, but 8-Br-cGMP failed to produce any change in current amplitude at concentrations as high as 1 mM. In a more recent study, however, NO donors were found to inhibit macroscopic N-type currents in dorsal root ganglion neurons (Yoshimura et al., 2001). The apparent contradiction between these findings may be related to the experimental models used in the studies cited. First of all, the function and modulation of N channels are probably different in mammals and lower vertebrates, as also mentioned by Hirooka et al. (2000). As far as mammalian neurons are concerned, studies performed on rat brain and sympathetic ganglia have highlighted the existence of different variants of the α_{1B} subunit of N channels, each with distinct functional properties (Lin et al., 1999). Functionally distinct cGMP-dependent protein kinases have also been identified in neurons (Lohmann et al., 1997; Hofmann et al., 2000). They can be either soluble or anchored at the plasma membrane and reportedly mediate a wide range of biological effects. It is thus plausible that the type of NO-induced modulation of N channels observed in a given experimental model depends in part on the specific N channel and G-kinase isoforms expressed in the preparation. Our data and those of Yoshimura et al. (2001) suggest, however, that the predominant effect of NO on the N channels in mammalian neurons is inhibitory, and this conclusion is consistent with the reported effects of this nonconventional transmitter on other HVA Ca^{2+} channel types.

It is interesting to consider the inhibition of N channels induced by the novel intercellular messenger NO in the context of the widely recognized and documented modulation of these channels by different classical neurotransmitters. Evidence has been accumulating that neurotransmitters induce voltage-dependent as well as voltage-independent modulation of calcium channels (Marchetti et al., 1986; for review, see Tsien et al., 1988; Carbone and Swandulla, 1989; Dolphin, 1995, 1998; Zamponi et al., 1997; Dunlap and Ikeda, 1998). G-protein-mediated inhibition of these channels is characterized by a slowing of the current activation kinetics, which has been attributed to a time-dependent recovery from voltage-dependent inhibition (Bean, 1989). Strong membrane depolarizations can overcome this inhibitory effect by Ca^{2+} channel facilitation consisting of changes in channel gating (Grassi and Lux, 1989; Elmslie et al., 1990; Delcour and Tsien, 1993; Carabelli et al., 1996; Lee and Elmslie, 2000). In light of these findings, it is conceivable that the nonconventional transmitter NO might contribute in some manner to the downregulation of N channel Ca^{2+} influx induced by classical neurotransmitters. NO differs from the latter molecules in terms of the mechanisms and channel sites of its action, and its effects are mediated by different second messengers. Nonetheless, the control of Ca^{2+} flux through neuronal membrane probably involves their functional cooperation. The NO/cGMP/PKG action reported in the present paper might thus represent a functionally relevant component of the complex mechanism regulating neurotransmitter release from nerve endings. Various types of HVA Ca^{2+} channels are known to be involved in neurotransmitter release, with the contribution of N channels usually ranging from 20 to 30% (for review, see Dunlap et al., 1995; Catterall, 1998; Grassi et al., 1999b). In postganglionic sympathetic fibers, N channels are primarily responsible for catecholamine release, and NO has been reported to inhibit both noradrenaline release from sympathetic nerve terminals and the vasoconstrictor response to adrenergic nerve stimulation (Tesfamariam et al., 1987; Greenberg et al., 1989). Moreover, the SNP/cGMP/PKG pathway has been considered responsible for inhibition of glutamate release in rat hippocampal nerve terminals (Sequeira et al., 1999). There is also evidence suggesting that NO can facilitate neurotransmitter release in some experimental models (Prast and Philippu, 1992; Herring and Paterson, 2001). It should be recalled, however, that in addition to its action on HVA Ca^{2+} channels, NO also enhances calcium release from intracellular stores (Willmott et al., 1995; Stoyanovsky et al., 1997), and the net result of these potentially contrasting effects may well depend on the experimental model used.

NO can be expected to exert its effects on N channels under a number of physiological and pathophysiological conditions that are associated with activation of NO synthase (NOS). This enzyme is widespread in both the CNS and PNS, and it has been identified in neurons as well as in glial cells [see references in Schuman and Madison (1994) and Rand and Li (1995)]. Three different NOS isoforms have been described: neuronal and endothelial NOS, which are specifically activated by various biological signals that increase intracellular Ca^{2+} levels, and the calcium-independent inducible isoform, the expression of which is induced by proinflammatory or ischemic stimuli [see references in Wiesinger (2001)]. In addition to that produced by nervous and glial cells themselves, NO synthesized and released by vascular endothelium can also spread to neurons and affect their functions.

In conclusion, the data discussed above suggest that the NO-induced modulation of N-type channels reported in the present paper may play a significant functional role in all biological functions that are regulated by changes in calcium influx through plasma membrane and, above all, in the control of neurotransmitter release in both the CNS and PNS.

REFERENCES

Azzena GB, Ferraresi A, Filippi GM, Grassi C, Manni E, Troiani D (2000) Proprioceptive afferents from extraocular muscles and oculomotor control: functional role of nitric oxide. Pflügers Arch 439:R263.38.

Bates JN, Baker MT, Guerra R, Harrison DG (1991) Nitric oxide gener-

ation from nitroprusside by vascular tissue. Biochem Pharmacol 42:S157–S165.
Bean BP (1989) Neurotransmitter inhibition of neuronal calcium currents by changes in channel voltage dependence. Nature 340:153–156.
Bolotina VM, Najibi S, Palacino JJ, Pagano PJ, Cohen RA (1994) Nitric oxide directly activates calcium–dependent potassium channels in vascular smooth muscle. Nature 368:850–853.
Carabelli V, Lovallo M, Magnelli V, Zucker H, Carbone E (1996) Voltage-dependent modulation of single N-type Ca^{2+} channel kinetics by receptor agonists in IMR32 cells. Biophys J 70:2144–2154.
Carabelli V, D'Ascenzo M, Carbone E, Grassi C (2002) Nitric oxide inhibits neuroendocrine Ca_v1 L-channel gating via cGMP-dependent protein kinase in cell-attached patches of bovine chromaffin cells. J Physiol (Lond) 541:351–366.
Carbone E, Swandulla D (1989) Neuronal calcium channels: kinetics, blockade and modulation. Prog Biophys Mol Biol 54:31–58.
Carbone E, Sher E, Clementi F (1990) Ca currents in human neuroblastoma IMR32 cells: kinetics, permeability and pharmacology. Pflügers Arch 416:170–179.
Catterall WA (1998) Structure and function of neuronal Ca^{2+}-channels and their role in neurotransmitter release. Cell Calcium 24:307–323.
Chen C, Schofield GG (1995) Nitric oxide enhanced Ca^{2+} currents and blocked noradrenaline-induced Ca^{2+} current inhibition in rat sympathetic neurons. J Physiol (Lond) 482:521–531.
Chik CL, Liu QY, Li B, Karspinski E, Ho AK (1995) cGMP inhibits L-type Ca^{2+} channel currents through protein phosphorylation in rat pinealocytes. J Neurosci 15:3104–3109.
Delcour AH, Tsien RW (1993) Altered prevalence of gating modes in neurotransmitter inhibition of N-type calcium channels. Science 259: 980–984.
Dolphin A (1995) The G. L. Brown prize lecture. Voltage dependent calcium channels and their modulation by neurotransmitters and G-proteins. Exp Physiol 80:1–36.
Dolphin A (1998) Mechanisms of modulation of voltage-dependent calcium channels by G-proteins. J Physiol (Lond) 506:3–11.
Dunlap K, Ikeda SR (1998) Receptor-mediated pathways that modulate calcium channels. Semin Neurosci 9:198–208.
Dunlap K, Luebke JI, Turner TJ (1995) Exocytotic Ca^{2+} channels in mammalian central neurons. Trends Neurosci 18:89–98.
Elmslie KS (1997) Identification of single channels which underlie the N-type and L-type calcium current in bullfrog sympathetic neurons. J Neurosci 17:2658–2668.
Elmslie KS, Zhou W, Jones SW (1990) LHRH and GPT-gamma-S modify activation of N-type calcium currents in bullfrog sympathetic neurons. Neuron 5:75–80.
Garthwaite J, Southam E, Boulton CL, Nielsen EB, Schmidt K, Mayer B (1995) Potent and selective inhibition of nitric oxide-sensitive guanynyl cyclase by 1H-[1, 2, 4]oxadiazolo[4, 3-a]quinoxalin-1-one. Mol Pharmacol 48:148–188.
Grassi C, Magnelli V, Carabelli V, Sher E, Carbone E (1994) Inhibition of low- and high-threshold Ca^{2+}-channels of human neuroblastoma IMR32 cells by Lamber-Eaton myasthenic syndrome (LEMS) IgGs. Neurosci Lett 181:50–56.
Grassi C, Santarelli R, Nisticò S, Bagetta G, Azzena GB (1995) Possible modulation of auditory middle latency responses by nitric oxide in the inferior colliculus of anaesthetized rats. Neurosci Lett 196:213–217.
Grassi C, D'Ascenzo M, Valente A, Azzena GB (1999a) Ca^{2+} channel inhibition induced by nitric oxide in rat insulinoma RINm5F cells. Pflügers Arch 437:241–247.
Grassi C, Martire M, Altobelli D, Azzena GB, Preziosi P (1999b) Characterization of Ca^{2+}-channels responsible for K^+-evoked [^{3}H]noradrenaline release from rat brain cortex synaptosomes and their response to amyotrophic lateral sclerosis IgGs. Exp Neurol 159:520–527.
Grassi C, Martinotti G, D'Ascenzo M, Azzena GB (2000) Inhibitory action exerted by nitric oxide on N-type calcium channels, in human neuroblastoma IMR32 cells. Eur J Neurosci 12[Suppl 11]:27.
Grassi F, Lux HD (1989) Voltage-dependent GABA-induced modulation of calcium currents in chick sensory neurons. Neurosci Lett 105:113–119.
Greenberg S, Diecke FPJ, Peevy K, Tanaka TP (1989) The endothelium modulates adrenergic neurotransmission to canine pulmonary arteries and veins. Eur J Pharmacol 162:57–80.
Grider JR (1993) Interplay of VIP and nitric oxide in regulation of the descending relaxation phase of peristalsis. Am J Physiol 264:G334–340.
Haley JE, Dickenson AH, Schachter M (1992) Electrophysiological evidence for a role of nitric oxide in prolonged chemical nociception in the rat. Neuroscience 31:251–258.
Hamill OP, Marty A, Neher E, Sakmann B, Sigworth FJ (1981) Improved patch-clamp techniques for high-resolution current recording from cells and cell-free membrane patches. Pflügers Arch 391:85–100.
Herring N, Paterson JD (2001) Nitric oxide-cGMP pathway facilitates acetylcholine release and bradycardia during vagal nerve stimulation in the guinea-pig in vitro. J Physiol (Lond) 535 2:507–518.
Hirooka K, Kourennyi DE, Barnes S (2000) Calcium channel activation facilitated by nitric oxide in retinal ganglion cells. J Neurophysiol 83:198–206.
Hofmann F, Ammendola A, Schlossmann J (2000) Rising behind NO: cGMP-dependent protein kinases. J Cell Sci 113:1671–1676.
Hu H, Chiamvimonvat N, Yamagishi T, Marban E (1997) Direct inhibition of expressed cardiac L-type Ca^{2+} channels by *S*-nitrosothiol nitric oxide donors. Circ Res 81:742–752.
Kasai H, Aosaki T, Fukuda J (1987) Presynaptic Ca-antagonist omega-conotoxin irreversibly blocks N-type Ca-channels in chick sensory neurons. Neurosci Res 4:228–235.
Kemenes I, Kemenes G, Andrew RJ, Benjamin PR, O'Shea M (2002) Critical time-window for NO-cGMP-dependent long-term memory formation after one-trial appetitive conditioning. J Neurosci 22:1414–1425.
Kurenny DE, Moroz LL, Turner RW, Sharkey KA, Barnes S (1994) Modulation of ion channels in rod photoreceptors by nitric oxide. Neuron 13:315–324.
Lambert RC, Feltz A (1995) Maintained L-type Ca^{2+} channel activity in excised patches of PTX-treated granule cells of the cerebellum. J Neurosci 15:6014–6022.
Lang RJ, Harvey JR, McPhee GJ, Klemm MF (2000) Nitric oxide and thiol reagent modulation of Ca^{2+}-activated K^+ (BKCa) channels in myocytes of the guinea-pig *Taenia caeci*. J Physiol (Lond) 525:363–376.
Lee HK, Elmslie KS (2000) Reluctant gating of single N-type calcium channels during neurotransmitter-induced inhibition in bullfrog sympathetic neurons. J Neurosci 20:3115–3128.
Li Z, Chapleau MW, Bates JN, Bielefeldt K, Lee HC, Abboud M (1998) Nitric oxide as an autocrine regulator of sodium currents in baroreceptor neurons. Neuron 20:1039–1049.
Lin Z, Lin Y, Schorge S, Qian Pan J, Beierlein M, Lipscombe D (1999) Alternative splicing of a short cassette exon in α_{1B} generates functionally distinct N-type calcium channels in central and peripheral neurons. J Neurosci 19:5322–5331.
Lohmann SM, Vaandrager AB, Smolenski A, Walter U, De Jonge HR (1997) Distinct and specific functions of cGMP-dependent protein kinases. Trends Biochem Sci 22:307–312.
Marchetti C, Carbone E, Lux HD (1986) Effects of dopamine and noradrenaline on Ca channels of cultured sensory and sympathetic neurons of chick. Pflügers Arch 406:104–111.
Meriney SD, Gray DB, Pilar GR (1994) Somatostatin-induced inhibition of neuronal Ca^{2+} current modulated by cGMP-dependent protein kinase. Nature 369:336–339.
Prast H, Philippu A (1992) Nitric oxide releases acetylcholine in the basal forebrain. Eur J Pharmacol 216:139–140.
Rand MJ, Li CG (1995) Nitric oxide as a neurotransmitter in peripheral nerves: nature and mechanism of transmission. Annu Rev Physiol 57:659–682.
Ropero AB, Fuentes E, Rovira JM, Ripoll C, Soria B, Nadal A (1999) Non-genomic actions of 17β-oestradiol in mouse pancreatic β-cells are mediated by a cGMP-dependent protein kinase. J Physiol (Lond) 521 2:397–407.
Sequeira SM, Carvalho AP, Carvalho CM (1999) Both protein kinase G dependent and independent mechanisms are involved in the modulation of glutamate release by nitric oxide in rat hippocampal nerve terminals. Neurosci Lett 261:29–32.
Schuman EM, Madison DV (1994) Nitric oxide and synaptic function. Annu Rev Neurosci 17:153–183.
Stoyanovsky D, Murphy T, Anno PR, Kim YM, Salama G (1997) Nitric oxide activates skeletal and cardiac ryanodine receptors. Cell Calcium 21:19–29.
Summers BA, Overholt JL, Prabhakar NR (1999) Nitric oxide inhibits L-Type Ca^{2+} current in glomus cells of the rabbit carotid body via a cGMP-independent mechanism. J Neurophysiol 81:1449–1457.
Tesfamariam B, Weisbrod RM, Cohen RA (1987) Endothelium inhibits responses of rabbit carotid artery to adrenergic nerve stimulation. Am J Physiol 253:H792–798.
Tewari K, Simard JM (1997) Sodium nitroprusside and cGMP decrease Ca^{2+} channel availability in basilar artery smooth muscle cells. Pflügers Arch 433:304–311.
Tsien RW, Lipscombe DV, Madison DV, Bley KR, Fox AP (1988) Multiple types of neuronal calcium channels and their selective modulation. Trends Neurosci 11:431–438.
Waniishi Y, Inoue R, Morita H, Teramoto N, Abe K, Ito Y (1998) Cyclic GMP-dependent but G-kinase-independent inhibition of Ca^{2+}-dependent Cl-currents by NO donors in cat tracheal smooth muscle. J Physiol (Lond) 511:719–731.
Wiesinger H (2001) Arginine metabolism and the synthesis of nitric oxide in the nervous system. Prog Neurobiol 64:365–391.
Willmott NJ, Galione A, Smith PA (1995) Nitric oxide induces Ca^{2+} mobilization and increases secretion of incorporated 5-hydroxytryptamine in rat pancreatic β-cells. FEBS Lett 371:1981–1992.
Yoshimura N, Seki S, de Groat WC (2001) Nitric oxide modulates Ca^{2+} channels in dorsal root ganglion neurons innervating rat urinary bladder. J Neurophysiol 86:304–311.
Zamponi GW, Bourinet E, Nelson D, Nargeot J, Snutch TP (1997) Crosstalk between G proteins and protein kinase C mediated by the calcium channel α_1 subunit. Nature 385:442–446.